



EXPERIMENTAL STUDY OF MECHANICAL LOSSES OF SINGLE-CYLINDER SPARK-IGNITED ENGINE

Carlos A ROMERO, Edison HENAO, Juan RAMÍREZ

Universidad Tecnológica de Pereira

cromero@utp.edu.co, edisonhenao@utp.edu.co, juandaviramireza@utp.edu.co

In this study, the mechanical losses of a single-cylinder spark-ignited Robin EY15 engine were experimentally determined and analysed by the indicated method. The effects of the load and speed on the mechanical loss balance were also analysed. The tests were conducted on a test bench equipped with a DC motor generator at speeds between 1500 and 4800 min⁻¹ and three load levels of 25, 50, and 100%. The results showed that the mechanical efficiency ranges between 22.5% and 83.2% for the tested engine and the evaluated operation points, attaining the highest efficiency under the full load and 2100 min⁻¹. However, at this load level, the efficiency is reduced to 29% with the increase in the rotation speed. Concurrently, the pumping losses contribute up to 58.7% of the total losses, which indicates that their contribution is even higher than the sum of the other components under low load conditions. However, as the load increases, this contribution decreases to 18% for lower rotation regimes. In addition, the experimental results of the total mechanical losses were compared with some numerical correlations found in the literature. Finally, some empirical correlations were proposed for the mechanical efficiency calculation of the tested engine.

Keywords: Internal combustion engines; Friction losses; Pumping losses; Mechanical efficiency.

1. INTRODUCTION

Internal combustion engines (ICEs) are machines that convert chemical energy into mechanical work by the combustion process [1]. However, only approximately 25% of the chemical energy that enters an engine is transformed into useful work in the output shaft [2]. The remainder of the energy is dissipated as heat to the environment through the exhaust gases, cooling system, and engine housing.

Only a fraction of the energy provided by the fuel is transformed into work in the combustion chamber (indicated work). However, approximately 20% of the indicated work is required to overcome the engine mechanical losses when operating at full load or 100% when it operates at no load [3]. The mechanical performance of the engines presents rotational speed and load level dependence. The major contributors to the mechanical losses are the drive devices of the auxiliary systems, which account for 15–25% of the total mechanical losses, and the friction of all the kinematic pairs of the engine, accounting for 45–65% [4]. The latter, in turn, is mainly contributed by the Piston/rings group, accounting for 50–68% of the friction, the crankshaft, amounting to 25–35%, and the camshaft, accounting for 10–20% [5]. In addition, the pumping in the intake and exhaust phases contributes 15–30% of the total mechanical losses for diesel engines [4] and up to 50% for gasoline engines [5]. By reducing mechanical losses, it is possible to improve engine performance, reduce fuel consumption and CO₂ emissions, extend durability, and thus, reduce operating costs [2],

[6]–[9]. However, evaluating the techniques for reducing losses, such as development of lubricants with better tribological properties and friction modifiers, surface treatments with better finish, and engine downsizing, requires experimental tests, even when numerical methodologies are used [4], [7], [10],[11].

There are different techniques for experimentally determining the mechanical performance of ICEs. Some methods allow studying mechanical losses under motoring conditions. However, owing to the absence of combustion, the loads and temperatures differ from the real operating ones, affecting the lubrication regimes of the kinematic pairs [12]–[15]. By the indicated method, which is extensively used and considered to have high precision, total mechanical losses are determined during engine operation. Therefore, the thermal and tribological conditions correspond to the normal operation conditions (real conditions) [1], [12], [13], [16], allowing observation of the speed and load variations effects on the mechanical performance. In addition, pumping losses can be calculated by analysing the intake and exhaust processes in the indicated diagram [4], [17]. The minimum variables required to implement the indicated method are the in-cylinder pressure, torque in the output shaft, and angular crankshaft position [3], [11]–[13], [18],

Using the indicated method, several researchers determined the mechanical losses of ICEs. Skjoedt et al. [18] analysed the lubricating base, oil viscosity, and friction modifier effect on the mechanical losses and fuel consumption of a 2.5-L six-cylinder engine at two operation points (1500

min^{-1} –90% load and 3000 min^{-1} –20% load). Noorman et al. [12] reported loss reduction by the addition of friction modifiers in a six-cylinder engine during various electronically controlled operating routines. Tests were conducted at three engine speeds (1500, 2000, and 3000 min^{-1}) and loads between 1/12 and 3/4 of the throttle opening. Mufti [19] determined the total mechanical losses of a single-cylinder Ricardo-Hydra overhead camshaft engine. In that study, tests were conducted at speeds between 800 and 2000 min^{-1} and loads of 1/4 and 1/2 of the throttle opening. Moreover, the effects of oil viscosity, oil temperature, and friction modifiers on the losses were analysed. Cruz-Peragon et al. [3] determined the mechanical losses and mechanical performance of a single-cylinder diesel engine operating at speeds between 1600 and 2800 min^{-1} and a three-cylinder spark ignition engine operating at speeds between 2500 and 6000 min^{-1} under variation in the load. The results showed that under a constant load, their mechanical efficiency decreases as the speed increases. In contrast, at a constant speed, the mechanical efficiency increases with increasing loads. However, from the above study, it is impossible to conclude the behaviour or contribution of the pumping losses. Wakuri et al. [16] analysed the pumping losses of a single-cylinder engine by varying the speed and the load, concluding that the contribution of the pumping losses is 10–20% of the total mechanical losses and that they are affected mainly by the engine speed. However, the experiment was conducted in a diesel engine, where the pumping losses are not considerably affected by the load variation because it does not have a throttle body in the intake. In addition, the total mechanical losses were determined by the run-out method, which is utilized in the absence of combustion. Gish et al. [15] analysed the mechanical performance, friction, and pumping losses of a four-cylinder spark ignition engine under two compression ratios (7:1 and 12:1) and five loads (3, 25, 50, 75, and 100%). The results showed that for a constant regime, the load increase and a higher compression ratio increase the in-cylinder pressure causes a greater friction from the in-cylinder pressure increase. This, in turn, produces a larger contact force in each kinematic pair of the crank–piston mechanism. Although, the mechanical efficiency was enhanced and the pumping losses were decreased owing to the reduction in the restrictions caused by the throttle valve at higher loads, this study was conducted at 1600 min^{-1} only.

Numerical study of the mechanical losses is a cost-effective alternative, which makes it possible to predict the losses by empirical correlations based on engine operating characteristics, such as the crankshaft speed, average piston speed, pressure in the intake duct, maximum in-cylinder pressure, and main engine measures [14], [20]–[22]. In addition, numerical studies involve mathematical modelling based on

the engine dynamics, kinematics, and tribological behaviour [4], [9], [11], [20], [21], [25] or application of black box models trained only with experimental data [10]. It should be clarified that the calibration of a model is subject to the particular characteristics of the engine.

In the present study, the total mechanical losses, pumping losses, sum of the friction and auxiliaries, and mechanical efficiency of a single-cylinder spark ignition engine were determined and analysed using the indicated method under varying rotation speeds and loads. Furthermore, the experimental results were compared to those calculated using some correlations available in the literature. Finally, a few empirical correlations were proposed to determine the mechanical efficiency of the tested engine. The characteristics and configuration of the implemented test bench, test protocol, and acquisition and processing information are presented below.

2. METHODOLOGY

The following sections briefly describe the equipment used and the test bench configuration for achieving the technically acceptance of the installed instrumentation technically acceptable. Some instruments used were uncertified, and so, were characterized in university laboratories. The procedures for the execution of the test, data acquisition, and mechanical loss calculation using the indicated method are described. In the final section, some numerical correlations available in the literature for mechanical loss prediction are described, to which the experimental results were compared.

2.1. Equipment and measuring instruments

This section presents the technical characteristics of the Robin EY15 engine, motor generator, and load system resistance bank in Table 1. The technical data of the instrumentation and the data acquisition system are summarized in Tables 2 and 3, respectively. The in-cylinder and intake pressure values reported in this work are manometric.

2.2. Test bench configurations

This section presents the integration of the test bench. The Robin EY15 engine, a torque metre, and motor-generator shafts were coupled, as shown in Figure 1. The intake duct was extended, and a large-volume tank was installed to suppress the intake air pulsations and improve the inlet mass flow measurement. The measuring instruments were installed at the illustrated locations, and the information was transferred to the corresponding signal acquisition system. The data were stored in a computer, except the engine fuel consumption, which was determined by measuring using a chronometer as the time to consume a known volume of fuel contained in a burette.

Table 1. Technical data of Robin EY15 engine and load system.

Robin EY15 engine	
Type	vertical, single-cylinder, side valve, spark ignited, air cooled
Bore x Stroke	63 mm x 46 mm
Displacement	143 cm ³
Compression ratio	6,3:1
Max power	2,6 kW at 4000 min ⁻¹
Max torque	6,7 Nm at 2800 min ⁻¹
Min fuel consumption	380 g/kWh
Lubrication type	splash
Oil (Quantity)	10W40 (600 ml)
Fuel system	Horizontal carburettor
Aspiration type	Naturally
Fuel	Gasoline
Motor generator	
Brand/series	pacific scientific/ SR series
Type	DC permanent magnet
Voltage/current	120 V/8,7A
Rotation speed	3200 min ⁻¹
Max power	2.0 HP
Electrical resistance bank	
Loads	20 fixed electrical resistance values
Max current	25 A

Table 2. Technical data of measuring instruments.

Device	Range	Sensibility	Resolution
Kistler 7061B pressure sensor	0-250 bar	-80 pC/bar	
kistler 5165A charge amplifier	0-10 V (output)	0,04 V/bar	
Futek TRS705 torque sensor with rotary encoder	± 50 Nm	0,1 V/Nm	1° (encoder)
IHH500 torque processor	0-5 V (output)	0,1 V/Nm	
Omron rotary encoder	720 P/R		0,5°
MAP sensor	10-300 kPa	0,053 V/kPa	
MAF sensor	<0,04 kg/s	non-linear response	
Burette	0-100 ml		1 ml
Chronometer			0,01 s
K type thermocouples	<1300 °C		

2.3. Experimental procedure

This section presents a simple description of the experimental phase and the signal acquisition procedure. The Robin EY15 engine tests were conducted under variable speeds between 1500 and 4800 min⁻¹ and loads of 25, 50, and 100% of the throttle opening. Because the resistance bank in the

load system has fixed values of electrical resistance, achieved by setting the position of the throttle valve, the speeds are not regulated, instead they are determined by the load system. The tested operation points are described in greater detail in Table 4. After setting each operation point, there was a waiting period of 2–3 min until the engine speed and different temperatures were stabilized. Regarding the data acquisition phase, two 10-s signals were captured, one each with NI9188 and NI6216 acquisition systems.

Table 3. Technical data of signal acquisition system.

Device	Data acquisition frequency	resolution	Acquired signals
NI 9188 DAQ	≤51,2 kS/s		
NI 9223	51,2 kS/s	16 bits	in-cylinder pressure, torque, MAF, MAP
NI 9211	10 S/s	24 bits	K type thermocouples
NI 6216	130 kS/s	16 bits	in-cylinder pressure, Omron encoder

Table 4. Test operating points.

Load	Rotation speed [min ⁻¹]
25%	1500, 1900, 2500, 2800
50%	1600, 2000, 2900, 3100, 3550, 4150, 4450, 4800
100%	2100, 3500, 4200, 4450, 4800

2.4. Mechanical losses calculation

The simple mathematical relationships used to calculate the ICE mechanical losses and its performance characteristics are presented in this section. In addition, the indicated method is described.

The mechanical losses are defined as the difference between the energy available in the piston by the combustion process and the useful energy obtained at the output shaft, and they are mathematically expressed by the following equations [1]:

$$W_m = W_i - W_e \quad (1)$$

where W_m : mechanical losses work, W_i : indicated work, and W_e : effective work.

The mechanical losses can also be expressed in terms of power using equation (2) and as mean effective pressures using equation (3).

$$\omega i W_m = \omega i (W_i - W_e) \rightarrow N_m = N_i - N_e \quad (2)$$

$$\frac{W_m}{V_d} = \frac{(W_i - W_e)}{V_d} \rightarrow FMEP = IMEP - BMEP \quad (3)$$

where ω : rotation frequency, i : cycle parameter (0,5 for 4T engine and 1 for 2T engine), N_m : mechanical loss power, N_i : indicated power, N_e :

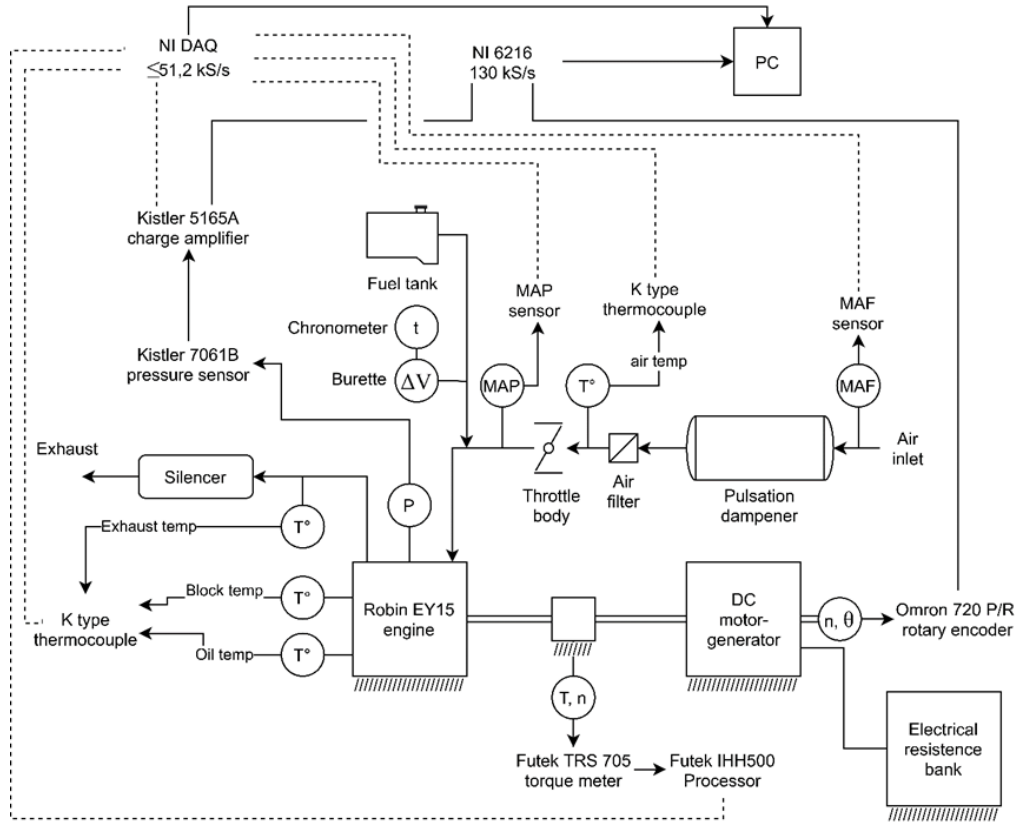


Fig. 1. Test bench scheme.

effective power, V_d : displacement, $FMEP$: friction mean effective pressure, $IMEP$: indicated mean effective pressure, and $BMEP$: brake mean effective pressure.

The mechanical efficiency is calculated using equation (4).

$$\eta_m = \frac{N_e}{N_i} \quad (4)$$

where η_m : mechanical efficiency.

The effective work and the BMEP are calculated by taking the average value of the torque signal during the 10-s data acquisition and using equation (6). The IMEP is calculated from the indicated diagram built by plotting the in-cylinder pressure, measured by a pressure sensor, versus the in-cylinder volume, calculated from the encoder signal. Figure 2 presents a representative indicated diagram showing the area corresponding to the indicated work, which is calculated using equation (5). The indicated method consists of calculating the mechanical losses causing the difference between the IMEP and BMEP. Using equation (5), the pumping work is calculated by integrating the area shown in Figure 2 and considering the closing angles of the intake and opening of the exhaust valves [4], [14]. Using this method, the pumping losses and the losses contributed by the friction and auxiliary contribution can be determined, as expressed in equation (7).

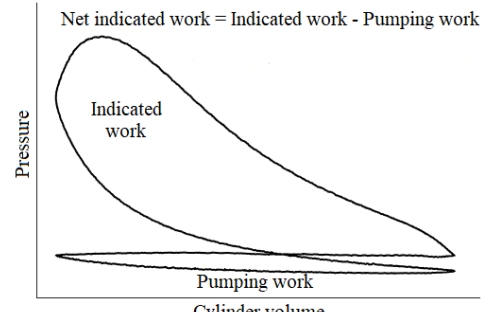


Fig. 2. Indicated diagram representation.

$$W_i = \int P dV \quad (5)$$

where W_i : indicated work, P : in-cylinder pressure, and V : in-cylinder volume.

$$W_e = \frac{2\pi T}{i} \quad (6)$$

where: W_e : effective work, T : output torque and i is 1 for 2T engines or 0,5 for 4T engines.

$$N_{fr+aux} = N_m - N_p \rightarrow RMEP + AMEP = FMEP - PMEP \quad (7)$$

where N_{fr+aux} : friction and auxiliary power losses, N_p : pumping loss power, $RMEP + AMEP$: sum of rubbing mean effective pressure and auxiliary mean effective pressure, and $PMEP$: pumping mean effective pressure.

The effective performance parameters were supplemented with the specific fuel consumption

and the net engine efficiency calculations using equations (8) and (9).

$$g_c = \frac{\dot{m}_{fuel}}{N_e} \quad (8)$$

where g_c : specific fuel consumption and \dot{m}_{fuel} : mass fuel flow.

$$\eta_e = \frac{N_e}{\dot{Q}_{fuel}} = \frac{N_e}{\dot{m}_{fuel} LHV} \quad (9)$$

where η_e : net engine efficiency, \dot{Q}_{fuel} : heat fuel flow, and LHV : lower heat value.

2.5. Comparative results

This section briefly describes four empirical correlations reported by other authors that allow the FMEP calculation from the geometric and operating characteristics of the engine. Gish et al. [15] conducted experimental measurements of a four-cylinder spark ignition engine under different loads and at a constant speed of 1600 min^{-1} , and found that the FMEP was only correlated to the maximum

in-cylinder pressure. Millington and Hartles [14] correlated the results of several diesel engine mechanical losses with different cylinder bores, the compression ratio, and the average piston speed. The tests were conducted under motoring conditions. The empirical correlations by Yagi et al. [20] and Fujii et al. [21] depend on the main dimensions of the engine (such as the piston bore and stroke), diameters and number of connecting rod and crankshaft journals, and rotation speed. They differ in that in the equation by Yagi et al., the effects of the intake valve flow area and the oil viscosity are accounted. In both the studies, the losses of motorcycle engines, including some ultrahigh-speed engines, were evaluated for different displacements, number and arrangements of cylinders, and maximum speed. The tests were conducted under motoring, fully open throttle valve, and exhaust manifold removal conditions. Table 5 lists the equations of the above-mentioned correlations.

Table 5. Correlations available in literature.

Gish et al.	$FMEP_{Pa} = 100000 + 0,0125 P_{max}$ P_{max} : maximum in-cylinder pressure in Pa
Millington & Hartles	$FMEP_{PSI} = A + \frac{7,0n}{1000} + 1,5 \left(\frac{V_{pf}}{1000} \right)^2$ A : compression ratio, V_{pf} : mean piston speed I ft/min, n : rotation regime min^{-1}
Fujii et al.	$FMEP_{MPa} = [3 \times 10^{-3} \cdot (n \times 10^{-3})^2 + 0,2] \frac{\sqrt{SD_m}}{B}$ S : stroke, B : bore, D_m : crankshaft equivalent diameter. $D_m = \frac{k_c \left[\sum_1^m D_{cj} + \sum_1^y D_{cp} \right]}{m + y}$ k_c : coefficient depending of cylinder number, D_{cj} : crank journal diameter, D_{cp} : crank pin diameter, m : number of crank journals, y : number of crank pins.
Yagi et al.	$FMEP_{MPa} = \left[60 \times 10^{-9} \cdot \left(\frac{V_c n}{z} \right)^2 + 1,1 \times 10^{-9} n^2 + 0,0011 \nu + 0,14 \right] \frac{\sqrt{SD_m}}{B}$ z : effective intake valve flow area m^2 , V_c : displacement in m^3 , ν : kinematic oil viscosity in cSt

3. RESULTS AND DISCUSSION

In the following sections, the experimental results of the effective performance, IMEP, and mechanical efficiency of the tested engine are discussed, and subsequently the pumping and friction and auxiliary contributions are analysed. The experimental results are compared with the calculated results based on the correlations in Table 5 by analysing the difference percentage. Finally, three empirical correlations are proposed to calculate the Robin EY engine mechanical efficiency from experimental data and are again compared to the experimental data.

3.1. Effective performance

In this section, the characteristics of the effective performance of the engine are discussed. Figure 3 shows the plots of the torque, power, specific fuel consumption, net efficiency, and BMEP for each load and tested rotation regime. It is observed that for a given speed, the load increase causes the torque, power, efficiency, and BMEP to increase. The maximum torque and the BMEP are 5.14 Nm and 4.5 bar , respectively, at 2100 min^{-1} . The maximum power is 1.77 kW at 4200 min^{-1} at full load, 1.02 kW at 2900 min^{-1} at 50% load, and 0.32 kW at 1500 min^{-1} at 25% load. This indicates that the maximum power is obtained at higher speeds as the load increases because of the ability the engine to deliver higher torques. It can be seen that as the load increases, the specific consumption

decreases; however, if the engine is accelerated to the fastest speed, the specific fuel consumption tends to increase, particularly for partial loads. This can be explained by the fact that the effective power drops rapidly at the highest speed and the engine continues to consume a considerable amount of fuel. The minimum consumption is 403.3 g/kWh at 2900 min^{-1} . The maximum and minimum net efficiency are 0.208 (20.8%) and 0.03 (3%), respectively, which suggests that 79.2%–97% of the energy provided by the fuel is dissipated as heat at the tested operating points. The net efficiency decreases owing to the decrease in the effective power and increase in the fuel consumption as the regime increases under any load. The maximum power and the torque characteristics are lower than those reported by the manufacturer whereas the minimum specific fuel consumption is higher. The maximum net efficiency obtained is lower than those of some engines with similar specifications. However, it must be noted that the effects of wear, mismatch, additional restrictions on the intake air flow, and air/fuel mixture calibration at each operation point affect the engine performance.

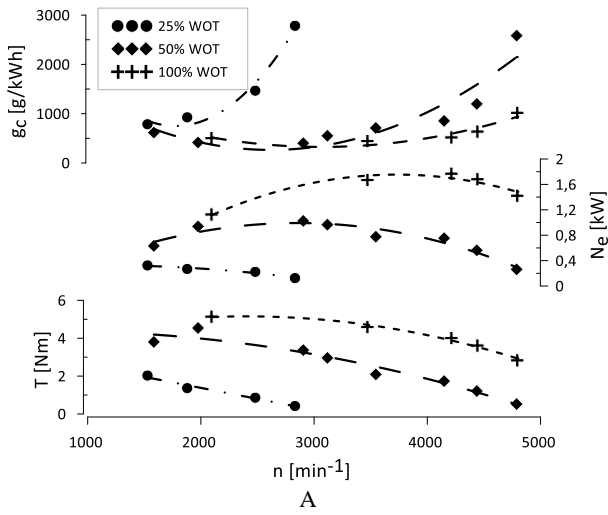
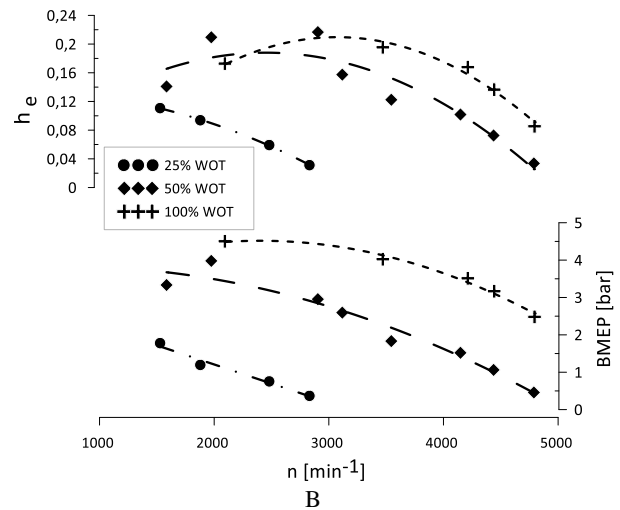


Fig. 3. Effective Robin EY15 engine performance, A. engine performance,

3.2. Indicated performance

In this section, the indicated parameters of the Robin EY15 engine are presented. The IMEP curves and P–V diagrams constructed for 25, 50, and 100% loads and a speed close to 2000 min^{-1} are shown in Figure 4. It can be seen that the IMEP increases because the in-cylinder pressure increase with the load, so that more work is obtained in each cycle. It can be seen that the IMEP, like BMEP, decreases with speed, varying from 5.41 bar at 2100 min^{-1} to 4.21 bar at 4800 min^{-1} under the full load conditions. This occurs owing to the rapid decrease in the torque required to drive the load system generator and the decrease in the volumetric engine efficiency. The pumping work area in the P–V diagram for 25% load is visibly larger than those for 50% and 100% load, which occurs mainly because the throttle valve position restricts the intake air flow and makes it difficult to fill the engine cylinder.



B. efficiency and BMEP.

3.3. Total mechanical losses

The engine mechanical performance plots and some operating conditions are shown below. Figure 5 shows the mechanical loss power, FMEP, mechanical efficiency, oil temperature, maximum in-cylinder pressure, and mean intake pressure. The power losses and FMEP increase mainly with the increase in the engine rotation speed. However, they slightly increase with the load caused by the in-cylinder pressure, which increases the friction forces between the rings, piston, and cylinder, particularly for speeds above 3000 min^{-1} . For tests performed at 25% load, the oil temperature is low; therefore, the viscosity is high and influences the losses reported for this load level. The engine FMEP varies from 0.91 bar at 2100 min^{-1} to 1.73 bar at 4800 min^{-1} under the full load conditions, and this range is similar to the FMEP values reported by Yagi et al. [20] and Fujii et al.

[21] for single-cylinder engines with similar displacements. However, there are some differences because their results were obtained from motoring tests and at oil temperatures close to $80\text{ }^{\circ}\text{C}$. It can be seen that the mechanical efficiency behaviour of the engine for a given speed improves with increasing load, reaching up to 83.2% at full load and 2100 min^{-1} . However, owing to the increase in the losses and the reduction in the effective power, the mechanical efficiency decreases as the speed increases, regardless of the load level, decreasing up to 59% at full load or up to 22.5% at partial loads. This suggests that the mechanical losses consume 16.8%–77.5% of the indicated power at the tested operation points. These values are close to the range of 22%–70% reported by Cruz-Peragon et al. [3] for a single-cylinder diesel engine at the tested operation points.

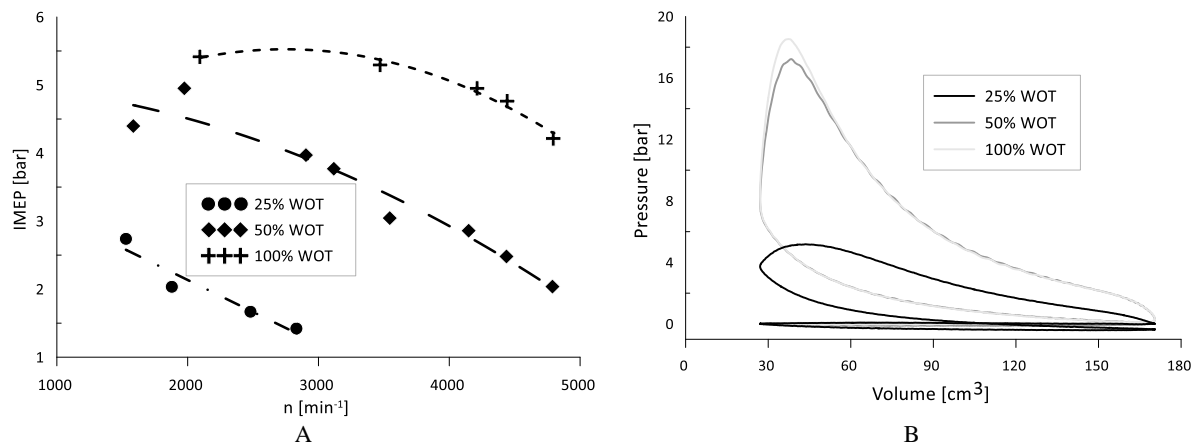
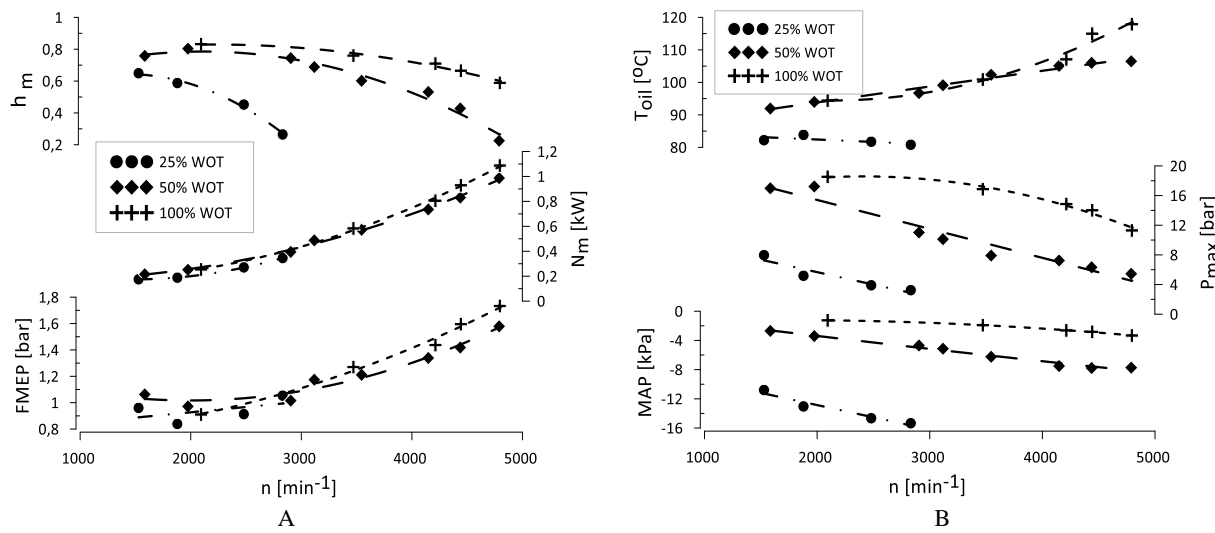
Fig. 4. Indicated performance. A. IMEP, B. P-V diagrams: 1900 min^{-1} 25%, 2000 min^{-1} 50% and 2100 min^{-1} 100%.

Fig. 5. Total mechanical losses, A. mechanical performance, B. operating conditions.

3.4. Mechanical loss components

This section presents the mechanical loss components obtained from the conducted experiments. In Figure 6, the curves of the power, mean effective pressure, and contributions of the pumping and friction and auxiliary loss components as percentages are shown. The pumping power increases with the rotation speed at any load level. However, it decreases with increasing load at a constant speed, which is related to the intake vacuum pressure increase with the air speed in the intake duct and decrease with the load caused by the throttle valve opening. Regarding the contribution of the PMEP over the FMEP, at full load, the pumping losses contribute between 18% at 2100 min^{-1} and 40.6% at 4200 min^{-1} . However, under partial loads, the PMEP contribution increases, reaching a maximum of 58.8% at 2500 min^{-1} and 25% load. This is higher than maximum PMEP contribution of 50% mentioned in the Wong and Tung review [5] and that of 38% reported by Gish et al. [15] at 1600 min^{-1} and 25% load for a four-cylinder spark ignition engine. However, it should be noted that the installed

pulsation damper reservoir restricts the air flow and produces a higher vacuum pressure. The friction and auxiliary contribution increases with the rotation speed and load increase, affected mainly by the in-cylinder pressure, which consequently intensifies the rings, pin, and piston skirt frictional force. The RMEP+AMEP over the FMEP contribution ranges between 82% at 2100 min^{-1} and 58.4% at 4200 min^{-1} at full load. However, at partial loads, the contribution decreases to 41.2% at 2500 min^{-1} and 25% load.

3.5. Correlations results

In this section, the experimentally obtained FMEP are compared with those calculated from the empirical correlations of other researchers. The calculated FMEP engine curves for different speeds and loads are presented in Figure 7. The Millington and Hartles [14] correlation shows the maximum difference from the experimental results, reaching a 94.7% error, because the correlation was obtained for diesel engines tested under motoring conditions

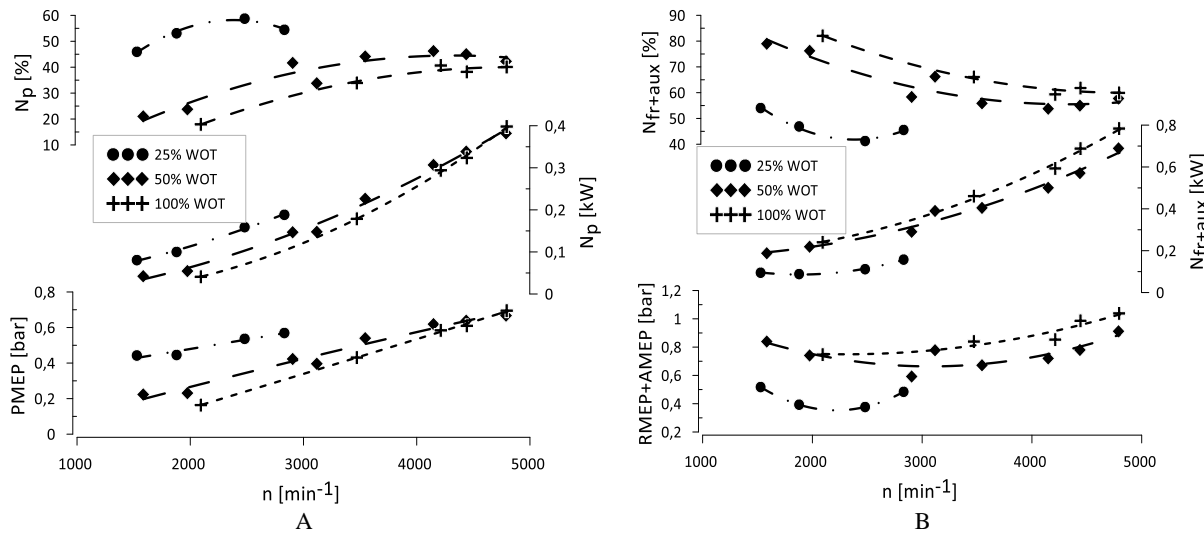


Fig. 6. Mechanical loss components. A. pumping, B. friction and auxiliaries.

and without a throttle valve. The Gish et al. [15] correlations is the best for 25% load, with differences ranging from 26.9% at 1900 min⁻¹ to 1.8% at 2800 min⁻¹. For 50% and 100% loads, the errors are lower than 32.3% and 34.2%, respectively. Based on the correlation of Yagi et al. [20], the errors are lower than 32.8%, 23.4%, and 18.24% for 25, 50, and 100% load levels, respectively. Finally, the Fujii et al. [21] correlation presents errors lower than 34.2%, 18.6%, and 25.2% for 25, 50, and 100% load levels, respectively. The last two methods are better adjusted for rotation speeds higher than 3500 min⁻¹ at full load, where the error is lower than 14.6%, possibly because their conditions are the most similar to those tested in the current experimental study.

3.6. Proposed mechanical efficiency correlations

This section presents three-dimensional graphs of the mechanical efficiency as a function of the speed, BMEP, maximum in-cylinder pressure, and mean intake pressure, and surfaces fitted to the plotted points are also displayed in each graph. Finally, the surface equations are used to calculate the FMEP, and the computed values are compared with the experimental results. The surface graphs of the mechanical performance are shown in Figure 8.

The plots show that the mechanical performance decreases as the rotation speed increases. However, it improves with the increase in the BMEP, maximum in-cylinder pressure, and mean intake pressure, which are variables modified by varying the load. Equations (10)–(12) correspond to the illustrated surfaces, and the R² value of each one is presented.

$$\begin{aligned} \eta_m = & 0,2594 + 0,2801BMEP + 1,605 \times 10^{-5}n \\ & - 0,03562BMEP^2 + 7,162 \times 10^{-7}nBMEP \quad (10) \\ & - 9,716 \times 10^{-9}n^2 \quad R^2 = 0,9764 \end{aligned}$$

$$\begin{aligned} \eta_m = & 0,08982 + 0,09114P_{max} + 6,083 \times 10^{-5}n \\ & - 3,356 \times 10^{-3}P_{max}^2 + 3,547 \times 10^{-6}nP_{max} \quad (11) \\ & - 2,616 \times 10^{-8}n^2 \quad R^2 = 0,9511 \end{aligned}$$

$$\begin{aligned} \eta_m = & 0,4763 - 0,03213MAP + 2,421 \times 10^{-4}n \\ & - 1,343 \times 10^{-3}MAP^2 + 1,674 \times 10^{-5}nMAP \quad (12) \\ & - 3,858 \times 10^{-8}n^2 \quad R^2 = 0,9594 \end{aligned}$$

$$FMEP = BMEP \left(\frac{1 - \eta_m}{\eta_m} \right) \quad (13)$$

The comparison of the FMEP calculated with equation (13) and the proposed correlations and the experimentally obtained FMEP can be seen in Figure 9. Under 25% load, the correlations lead to error values less than 27.7%, 33.6%, and 19.2%. Under 50% load, they were less than 21.6%, 22.6%, and 32.7%, and under full load were less than 26.6%, 42.3%, and 19.5%, respectively, using equations (10)–(12), respectively. However, it should be noted that for 50% load at speeds between 2000 and 3550 min⁻¹, the errors are less than 8.7%, 12.2%, and 13.1%. Moreover, for speeds greater than 3500 min⁻¹ at full load, the errors are less than 6.1%, 8.5%, and 19.5%, with equations (10), (11), and (12), respectively. It should be noted that the correlations proposed in this section were obtained only from the Robin EY15 engine experimental results; therefore, they may need to be calibrated for other engine types.

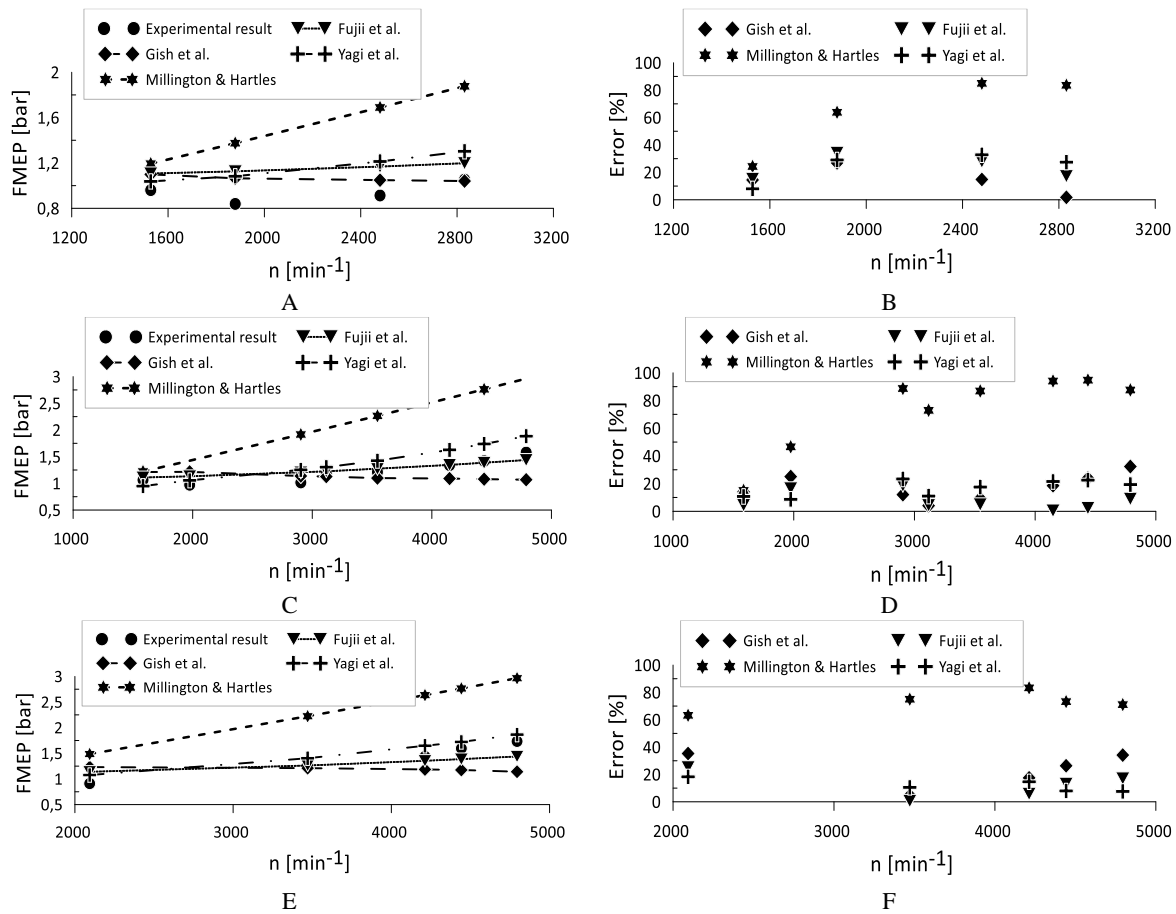


Fig. 7. FMEP correlations. A. 25% load, B. error percentage 25% load, C. 50% load, D. error percentage 50% load, E. 100% load, F. error percentage 100% load.

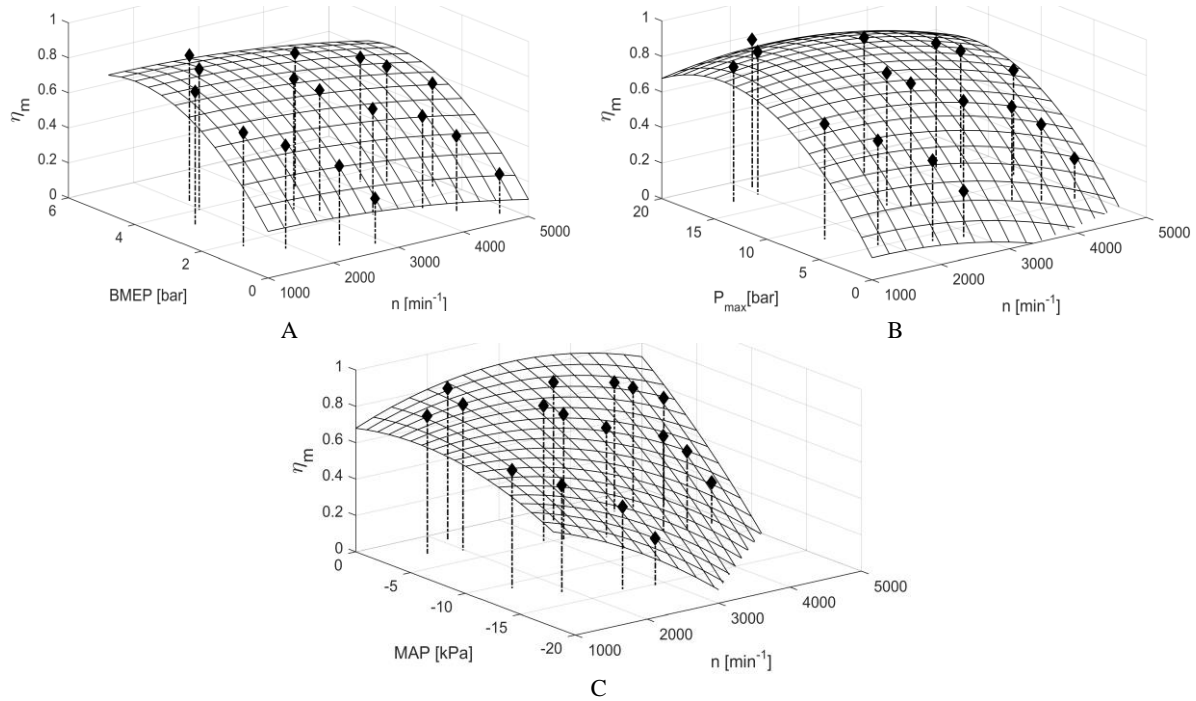


Fig. 8. Mechanical efficiency graphs in terms of rotation speed, A. BMEP, B. maximum in-cylinder pressure, C. mean intake pressure.

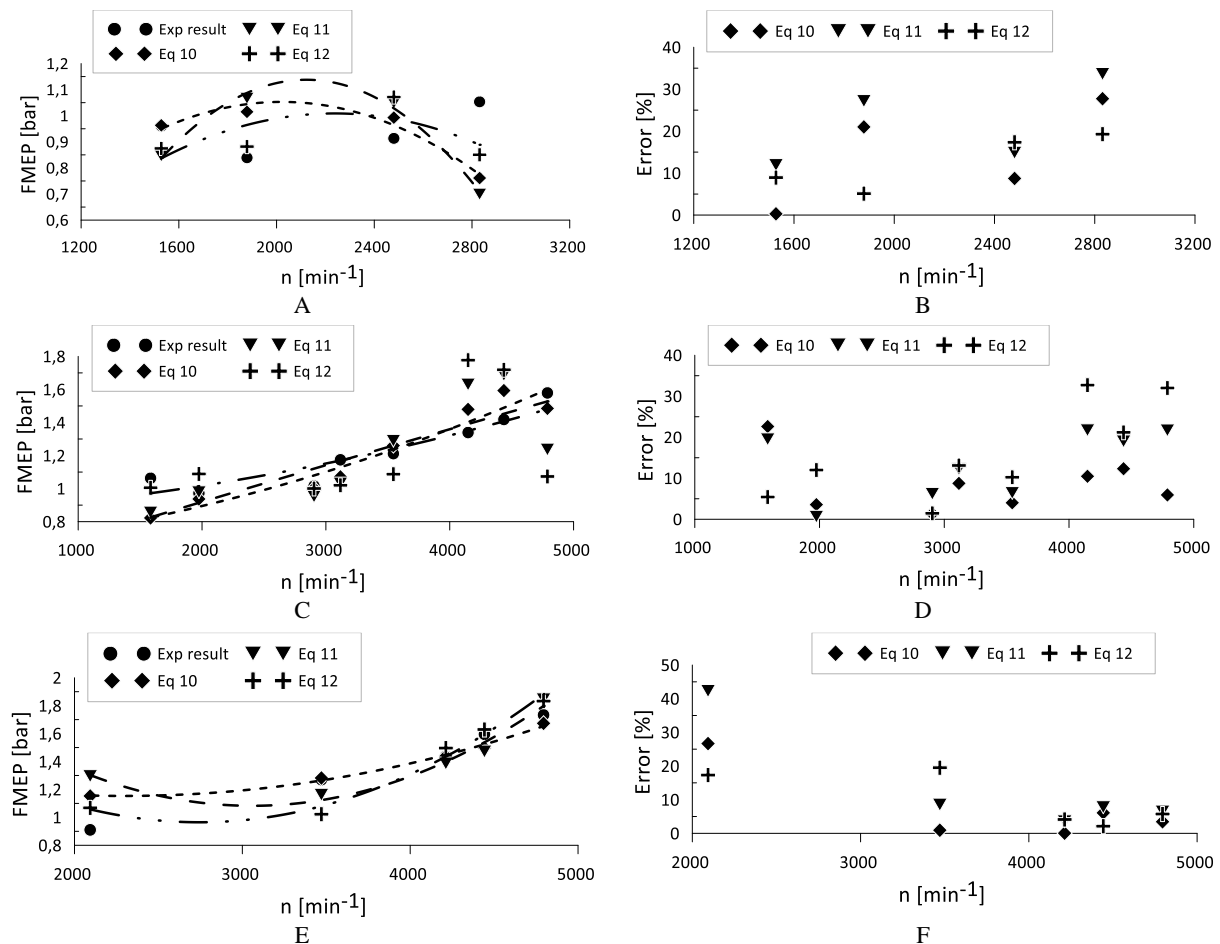


Fig. 9. FMEP calculated by proposed correlations. A. 25% load, B. error percentage 25% load, C. 50% load, D. error percentage 50% load, E. 100% load, F. error percentage 100% load.

4. CONCLUSIONS

The mechanical losses determined by the indicated diagram method and the contributions of the pumping and friction and auxiliary losses were characterized and analysed on a single-cylinder ICE Robin EY15 under different rotation speeds and loads.

The effective engine performance was characterized. The maximum torque and BMEP were 5.14 Nm and 4.5 bar at 2100 min⁻¹, respectively, and the maximum power was 1.77 kW at 4200 min⁻¹ at full load. The minimum specific fuel consumption was 403.3 g/kWh at 2900 min⁻¹. The maximum net efficiency was 0.208 (20.8%), and the minimum was 0.03 (3%); therefore, it was concluded that 79.2%–97% of the energy provided by the fuel is dissipated in the form of heat at the tested operation points.

The engine mechanical efficiency was determined. The engine FMEP ranges from 0.91 bar at 2100 min⁻¹ to 1.73 bar at 4800 min⁻¹ under the full load conditions. It was concluded that the FMEP represents 16.8%–77.5% of the IMEP for the evaluated operation points, which is used for overcoming the different losses.

The pumping losses contribution to the total mechanical losses was analysed. Under the full load

conditions, the PMEP contributes between 18% at 2100 min⁻¹ and 40.6% at 4200 min⁻¹ of the FMEP. However, the PMEP contribution increases, reaching a maximum of 58.8% of the FMEP at 2500 min⁻¹ and 25% load, which is higher than the maximum contribution mentioned in other referred studies. This is because the pulsation suppressor tank installed in the intake generates an additional air flow restriction, causing a higher vacuum pressure. However, the sum of the RMEP and AMEP contributions ranges between 82% and 41.2% of the FMEP, having greater relevance as the regime or load increases.

The experimental FMEP results were compared with those calculated using some correlations available in the literature. The error percentages were lower than 34.2%, 32.3%, and 26.3% for load levels of 25, 50, and 100%, respectively, using the Gish et al. [13], Fujii et al. [19], and Yagi et al. [18] correlations, respectively. It is clarified that the test conditions of the correlations were different from the Robin EY15 engine test conditions.

Three empirical correlations dependent on the rotation speed and variables sensitive to load variation, such as the BMEP, maximum in-cylinder pressure, and mean intake pressure, were obtained to determine the engine mechanical efficiency. The FMEP calculated using these correlations was

compared with the experimental FMEP. The error percentages were less than 33.6%, 32%, and 42.3% for load levels of 25%, 50%, and 100% using equations (10)–(12), respectively. However, for speeds between 2000 and 3550 min⁻¹ at 50% load, the error was less than 13.1%, and for speeds above 3500 min⁻¹ at full load, it was less than 19.5%.

ACKNOWLEDGEMENTS

The authors thank the Universidad Tecnológica de Pereira UTP (Technological University of Pereira) for their support throughout the research and to the Colombian “Departamento Administrativo de Ciencia, Tecnología e Innovación Colciencias” for supporting the project entitled: "Desarrollo de un sistema de monitoreo para el análisis energético y de condición de emisiones en motores de combustión interna diésel con base en técnicas no intrusivas" ("Development of a monitoring system for energy analysis and emission condition in diesel internal combustion engines based on non-intrusive techniques") code 1110-776- 57801, through which the research described in this article was developed.

REFERENCES

1. Heywood J. Internal combustion engine fundamentals. McGraw-Hill. 1988.
2. Tormos B, Ramírez L, Johansson J, Björpling M, Larsson R. Fuel consumption and friction benefits of low viscosity engine oils for heavy duty applications. *Tribology International*. 2017;110(6): 23–34. <http://dx.doi.org/10.1016/j.triboint.2017.02.007>
3. Cruz-Peragón F, Palomar J, Díaz F, Jiménez-Espadafor F. Fast on-line identification of instantaneous mechanical losses in internal combustion engines. *Mechanical Systems and Signal Processing*. 2010;24(1):267–280. <http://dx.doi.org/10.1016/j.ymssp.2009.06.009>
4. Tormos B, Martín J, Carreño R, Ramírez L. A general model to evaluate mechanical losses and auxiliary energy consumption in reciprocating internal combustion engines. *Tribology International*. 2018;123(7):161–179. <https://doi.org/10.1016/j.triboint.2018.03.007>
5. Wong V, Tung S. Overview of automotive engine friction and reduction trends—Effects of surface, material, and lubricant-additive technologies. *Friction*. 2016;4:1–28. <https://doi.org/10.1007/s40544-016-0107-9>
6. Sgroi M, Asti M, Gili F, Deorsola F, Bensaid S, Fino D, Kraft G, García I, Dassenoy F. Engine bench and road testing of an engine oil containing MoS₂ particles as nano-additive for friction reduction. *Tribology International*. 2017;105(1): 317–325. <http://dx.doi.org/10.1016/j.triboint.2016.10.013>
7. Thring RH. Engine friction modeling. *SAE Technical Paper*. 1992;(0920482). <https://doi.org/10.4271/920482>
8. Kumar V, Sinha S, Agarwal A. Tribological studies of an internal combustion engine. In: Agarwal A, Gupta J, Sharma N, Singh A. (eds) Advanced engine diagnostics. Energy, Environment, and Sustainability. Springer, Singapore; 2019. https://doi.org/10.1007/978-981-13-3275-3_12
9. Tormos B, Martín J, Pla B, Jiménez-Reyes A. A methodology to estimate mechanical losses and its distribution during a real driving cycle. *Tribology International*. 2020;145(5):106208. <https://doi.org/10.1016/j.triboint.2020.106208>
10. Arsie I, Pianese C, Rizzo G, Flora R, Serra G. Development and validation of a model for mechanical efficiency in a spark ignition engine. *SAE Technical Paper*. 1999; (1999-01-0905). <https://doi.org/10.4271/1999-01-0905>
11. Fang C, Meng X, Xie Y, Wen C, Liu R. An improved technique for measuring piston-assembly friction and comparative analysis with numerical simulations: Under motored condition. *Mechanical Systems and Signal Processing*. 2019;115:657–676. <https://doi.org/10.1016/j.ymssp.2018.06.015>
12. Norman M, Assanis D, Patterson DJ. Overview of techniques for measuring friction using bench tests and fired engines. *SAE Technical Paper*. 2000; (2000-01-1780). <https://doi.org/10.4271/2000-01-1780>
13. Koch F, Geiger U, Hermen F. PIFFO - Piston friction force measurements during engine operation. *SAE Technical Paper*. 1996; (960306). <https://doi.org/10.4271/960306>
14. Millington B, Hartles E. Frictional losses in diesel engines. *SAE Technical Paper*. 1968; (680590). <https://doi.org/10.4271/680590>
15. Gish R, McCullough J, Retzlaff J, Mueller H. Determination of true engine friction. *SAE Technical Paper*. 1958;(580063). <https://doi.org/10.4271/580063>
16. Wakuri Y, Soejima M, Ejima Y, Hamatake T, Kitahara T. Studies on friction characteristics of reciprocating engines. *SAE Technical Paper*. 1995; (952471). <https://doi.org/10.4271/952471>
17. Shelby M, Stein R, Warren C. A new analysis method for accurate accounting of IC engine pumping work and indicated work. *SAE Technical Paper*. 2004; (2004-01-1262). <https://doi.org/10.4271/2004-01-1262>
18. Skjoeidt M, Butts R, Assanis DN, Bohac S V. Effects of oil properties on spark-ignition gasoline engine friction. *Tribology International*. 2008;41(6):556–563. <https://doi.org/10.1016/j.triboint.2007.12.001>
19. Mufti R. Total and Component Friction in a Motored and Firing Engine. 2004.
20. Yagi S, Ishibashi Y, Sono H. Experimental analysis of total engine friction in four stroke S. I. engines. *SAE Technical Paper*. 1990; (900223). <https://doi.org/10.4271/900223>
21. Fujii I, Yagi S, Sono H, Kamiya H. Total Engine Friction in Four Stroke SI Motorcycle Engine. *SAE Technical Paper*. 1988;(880268). <https://doi.org/10.4271/880268>
22. Ciulli E. Review of internal combustion engine losses. Part 2: Studies for global evaluations. *Proceedings of the Institution of Mechanical Engineers, Part D: Journal of Automobile Engineering*. 1993;207(3):229–240. https://doi.org/10.1243/PIME PROC 1993 207 18 4_02
23. Rezeka S, Henein N. A new approach to evaluate instantaneous friction and its components in internal combustion Engines. *SAE Technical Paper*. 1984; (840179). <https://doi.org/10.4271/840179>

24. Patton KJ, Nitschke RC, Heywood JB. Development and evaluation of a friction model for spark-ignition engines. SAE Technical Paper. 1989; (890836). <https://doi.org/10.4271/890836>
25. Lee S, Kang J, Park S. Measurement and modeling of crank train friction in light-duty diesel engines. Journal of Mechanical Science and Technology. 2020;34(2):889–903. <https://doi.org/10.1007/s12206-020-0139-y>

Received 20xx21-03-12

Accepted 2021-08-12

Available online 2021-08-13



Carlos ROMERO received Ph.D. degree in Mechanical Engineering from Valencia Polytechnic University, Valencia, Spain, in 2009. Now he works at Pereira Technological University. His current research interests include internal combustion machine, and machine design.



Edison HENAO received Ph.D. degree in Engineering from Pereira Technological University, Pereira, Colombia, in 2021. Now he works at Pereira Technological University. His current research interests include mechanisms analysis, Internal combustion machine, and machine design.



Juan RAMÍREZ received Mechanical Engineer degree from Pereira Technological University, Pereira, Colombia, in 2017. Now he works at Pereira Technological University and he is Mechanical Engineering M.Sc. student at Pereira Technological University. His current research interests include Internal combustion machine, and machine design.